

# Therapeutic Efficacy of a Bivalent Inhibitor of Prostate-Specific Membrane Antigen Labeled with $^{67}\text{Cu}$

Lachlan E. McInnes<sup>1</sup>, Carleen Cullinane<sup>2</sup>, Peter D. Roselt<sup>3</sup>, Susan Jackson<sup>2</sup>, Benjamin J. Blyth<sup>2</sup>, Ellen M. van Dam<sup>4</sup>, Nicholas A. Zia<sup>1</sup>, Matthew J. Harris<sup>4</sup>, Rodney J. Hicks<sup>\*2,3</sup>, and Paul S. Donnelly<sup>\*1</sup>

<sup>1</sup>School of Chemistry, Bio21 Molecular Science and Biotechnology Institute, University of Melbourne, Parkville, Victoria, Australia; <sup>2</sup>Sir Peter MacCallum Department of Oncology, University of Melbourne, Parkville, Victoria, Australia; <sup>3</sup>Cancer Imaging, Peter MacCallum Cancer Centre, Melbourne, Victoria, Australia; and <sup>4</sup>Clarity Pharmaceuticals Ltd., Eveleigh, New South Wales, Australia

Radionuclide therapy targeting prostate-specific membrane antigen (PSMA) is promising for prostate cancer. We previously reported a ligand,  $^{64}\text{Cu}$ -CuSarbisPSMA, featuring 2 lysine-ureido-glutamate groups. Here, we report the therapeutic potential of  $^{67}\text{Cu}$ -CuSarbisPSMA. **Methods:** Growth of PSMA-positive xenografts was evaluated after treatment with  $^{67}\text{Cu}$ -CuSarbisPSMA or  $^{177}\text{Lu}$ -LuPSMA imaging and therapy (I&T). **Results:** At 13 d after injection, tumor growth was similarly inhibited by the 2 tracers in a dose-dependent manner. Survival was comparable after single (30 MBq) or fractionated ( $2 \times 15$  MBq, 2 wk apart) administrations. **Conclusion:**  $^{67}\text{Cu}$ -CuSarbisPSMA is efficacious in a PSMA-expressing model of prostate cancer.

**Key Words:**  $^{64}\text{Cu}$ ;  $^{67}\text{Cu}$ ; theranostics; prostate cancer; prostate-specific membrane antigen

**J Nucl Med 2021; 62:829–832**  
DOI: 10.2967/jnumed.120.251579

Prostate-specific membrane antigen (PSMA) is a membrane-bound enzyme that can act as a glutamate carboxypeptidase or folate hydrolase. In prostate cancer cells, it becomes membrane-bound and overexpressed with androgen independence and metastasis (1), making it a promising target for both imaging and therapy (2). Radiolabeled peptidomimetic inhibitors of PSMA containing a lysine-ureido-glutamate functional group are effective tracers for imaging prostate cancer using PET (2–4). A theranostic paradigm involves PET with Glu-NH-CO-NH-Lys-(Ahx)-*N,N'*-bis-[2-hydroxy-5-(carboxyethyl)benzyl]ethylenediamine-*N,N'*-diacetic acid labeled with  $^{68}\text{Ga}$  (half-life, 68 min; mean  $\beta^+$  energy, 0.89 MeV) ( $^{68}\text{Ga}$ -GaPSMA-11) to guide therapy with  $^{177}\text{Lu}$ -LuPSMA-617 (half-life, 6.65 d;  $\beta^-$ , 100%; mean  $\beta^-$  energy, 134 keV) (5–7). This approach has allowed personalized treatment of advanced prostate cancer, but the short half-life of  $^{68}\text{Ga}$  limits the ability to do prospective dosimetry (8), as does the use of differing ligands for diagnosis and therapy. Use of the DOTAGA-containing urea-based PSMA inhibitor called PSMA imaging and therapy (I&T), which can be labeled with either  $^{68}\text{Ga}$  or  $^{177}\text{Lu}$ , or use of  $^{68}\text{Ga}$ -GaPSMA-617 in place of  $^{68}\text{Ga}$ -GaPSMA-11 (5,9,10) can overcome

the latter limitation, but both approaches remain constrained for prospective dosimetry. Both limitations could be potentially addressed by using the positron-emitting ( $\beta^+$ )  $^{64}\text{Cu}$  (half-life, 12.7 h;  $\beta^+$ , 17.4%; mean  $\beta^+$  energy, 278 keV) for diagnosis and  $\beta^-$ -emitting  $^{67}\text{Cu}$  (half-life, 61.9 h;  $\beta^-$ , 100%; mean  $\beta^-$  energy, 141 keV) for therapy. The  $\beta^-$  emissions of  $^{67}\text{Cu}$  have a mean range of 0.2 mm and are appropriate for the treatment of small tumors down to 5 mm in diameter (11). The  $\gamma$  emission of  $^{67}\text{Cu}$  (185 keV, 49%; 93 keV, 16%) may be beneficial for quantitative SPECT to verify the radiation dose to the tumor and critical organs (12). The efficacy of targeted therapy with  $^{67}\text{Cu}$  has been demonstrated previously in non-Hodgkin lymphoma and neuroendocrine tumors (11,13,14).

The potential advantages of copper radiopharmaceuticals are dependent on high retention in tumors and clearance from normal tissues. The use of chelators that form copper complexes susceptible to release of copper in vivo can lead to high liver uptake at late time-points (15). Importantly, copper(II) complexes of sarcophagine (Sar = 3,6,10,13,16,19-hexa-azabicyclo[6.6.6]icosane)-based ligands are stable in vivo (16). A Sar derivative conjugated to a somatostatin receptor-targeting peptide,  $^{64}\text{Cu}$ -CuSarTATE, allows acquisition of high-quality images at 24 h after injection in patients with neuroendocrine tumors (16), and its therapeutic partner,  $^{67}\text{Cu}$ -CuSarTATE, is highly efficacious in a neuroendocrine tumor model (14). We recently reported high tumor uptake and retention of a  $^{64}\text{Cu}$ -labeled sarcophagine ligand tethered to 2 lysine-ureido-glutamate functional groups in a PSMA-positive model (17). In the current study, we evaluated the therapeutic efficacy of its  $^{67}\text{Cu}$ -labeled partner,  $^{67}\text{Cu}$ -CuSarbisPSMA (Fig. 1), in the same PSMA-positive tumor model.

## MATERIALS AND METHODS

### Radiochemistry

To synthesize  $^{67}\text{Cu}$ -SarbisPSMA,  $^{67}\text{Cu}$ -CuCl<sub>2</sub> (756 MBq, 70  $\mu\text{L}$ , 0.05 M HCl; Idaho State University) was added to a mixture of SarbisPSMA (AusPep) (17) (20  $\mu\text{g}$ , 10 nmol, in 10  $\mu\text{L}$  of 50:50 ethanol:water) and sodium phosphate buffer (0.1 M, pH 6.2, 350  $\mu\text{L}$ ). After 10 min at room temperature, analysis by high-performance liquid chromatography indicated at least 95% radiochemical purity (72 GBq/ $\mu\text{mol}$ ; retention time, 10.9 min; precursor retention time, 11.0 min). The high-performance liquid chromatography was performed on a Shimadzu SPD-10ATvP chromatograph using a Phenomenex Luna C18 100Å column (4.6  $\times$  150 mm, 5  $\mu\text{m}$ ) at a rate of 1 mL/min (5%–100% acetonitrile; 0.05% trifluoroacetic acid) over 15 min.

$^{177}\text{Lu}$ -LuPSMA I&T was prepared according to published procedures in at least 95% radiochemical yield using PSMA I&T (200  $\mu\text{g}$ ,

Received Jun. 15, 2020; revision accepted Sep. 17, 2020.  
For correspondence or reprints, contact Paul S. Donnelly (paul@unimelb.edu.au) and Rodney J. Hicks (Rod.Hicks@petermac.org).  
\*Contributed equally to this work.  
Published online Oct. 16, 2020.  
COPYRIGHT © 2021 by the Society of Nuclear Medicine and Molecular Imaging.

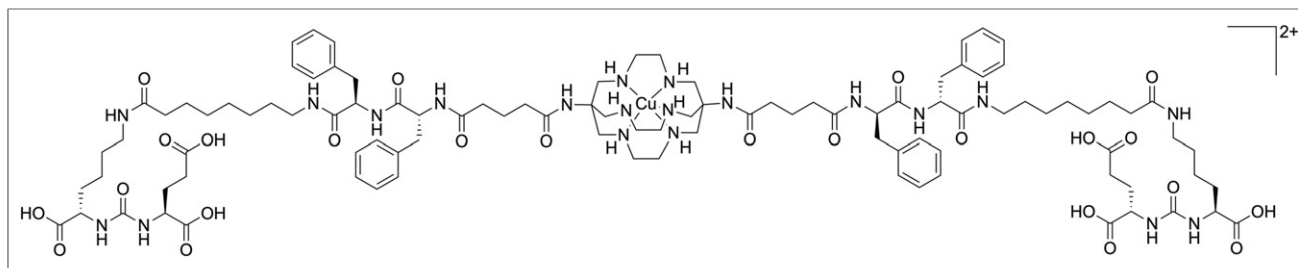


**FIGURE 1.** Chemical structure of  $^{64/67}\text{Cu}$ -CuSarbisPSMA.

0.13  $\mu\text{mol}$ ) (ABX) and  $^{177}\text{LuCl}_3$  (8 GBq) (ANSTO) (58 GBq/ $\mu\text{mol}$ ) (5).

### In Vivo Comparative Experiment

All animal experiments were performed with the approval of the institutional animal ethics committee. Eight-week old male NSG mice (Australian BioResources) were implanted with LNCaP (human prostate adenocarcinoma) cells as described previously (17). Mice ( $n = 5$ ) bearing subcutaneous LNCaP xenografts (mean tumor volume,  $\sim 90 \text{ mm}^3$ ) were randomized into 5 groups and injected intravenously with vehicle (saline),  $^{67}\text{Cu}$ -CuSarbisPSMA (5 or 30 MBq), or  $^{177}\text{Lu}$ -LuPSMA I&T (5 or 30 MBq) on day 1 of the experiment. Tumor size and health were monitored twice weekly, with mice being euthanized when tumor volume (calculated as length  $\times$  width  $\times$  height [mm]  $\times \pi/6$ ) exceeded  $1,200 \text{ mm}^3$ .

### In Vivo Dose-Dependency Experiment

Male NSG mice ( $n = 8$  per group) with subcutaneous LNCaP xenografts (mean tumor volume,  $\sim 240 \text{ mm}^3$ ) were injected with either saline or  $^{67}\text{Cu}$ -CuSarbisPSMA (7.5, 15, or 30 MBq) on day 1 of the experiment. An additional cohort was injected with  $^{67}\text{Cu}$ -CuSarbisPSMA (15 MBq) on days 1 and 15 of the experiment ( $n = 8$ ) and monitored as above.

### Data Analysis

Percentage tumor growth inhibition was calculated as  $100 \times (1 - \Delta T/\Delta C)$ , where  $\Delta C$  and  $\Delta T$  were determined by subtracting the mean tumor volume (in the vehicle control and treated groups, respectively) on day 1 of treatment from the mean tumor volume on either day 17 for the comparative experiment or day 13 for the dose-dependency experiment. Statistical analysis was performed using Prism, version 8.0 (GraphPad). Statistical comparisons between the vehicle control and treated cohorts were done by a 1-way ANOVA followed by a

Dunnett post hoc test. Toxicity was assessed by body-weight loss and by physical and behavioral observation. The experiment was ended on day 82 or 85, with the remaining mice being censored for survival. Survival curves (tumor volume  $\geq 1,200 \text{ mm}^3$ ) were analyzed using the Mantel–Cox log-rank test.

## RESULTS

### $^{67}\text{Cu}$ -CuSarbisPSMA and $^{177}\text{Lu}$ -LuPSMA I&T Are Efficacious Against LNCaP Tumor Xenograft Model

$^{67}\text{Cu}$ -CuSarbisPSMA was prepared in high radiochemical purity ( $>95\%$ ) in sodium phosphate buffer without the need for further purification before injection. Mice bearing subcutaneous LNCaP tumors were randomized into groups of 5 animals (mean tumor volume,  $90 \text{ mm}^3$ ) and then injected with saline,  $^{67}\text{Cu}$ -CuSarbisPSMA (5 MBq, 0.06 nmol, or 30 MBq, 0.36 nmol), or  $^{177}\text{Lu}$ -LuPSMA I&T (5 MBq, 0.08 nmol, or 30 MBq, 0.48 nmol). The inhibition of tumor growth was similar for both agents after administration of both 5 and 30 MBq, but demonstrated dose dependency (Table 1; Fig. 2). Survival was increased significantly in the 30-MBq dose cohorts when compared with the cohorts treated with 5 MBq ( $P = 0.002$  for both agents) (Fig. 2B).

### Inhibition of LNCaP Tumor Growth Is Dependent on the Activity of $^{67}\text{Cu}$ -CuSarbisPSMA Administered

Mice were inoculated with LNCaP cells and, once tumors were established, were randomized into 5 groups (mean tumor volume,  $240 \text{ mm}^3$ ) and intravenously injected with either saline or increasing doses of  $^{67}\text{Cu}$ -CuSarbisPSMA (7.5 MBq, 0.21  $\mu\text{g}$ , 0.1 nmol; 15 MBq, 0.45  $\mu\text{g}$ , 0.22 nmol; or 30 MBq, 0.89  $\mu\text{g}$ , 0.44 nmol) on day 1 of the experiment. An additional group was injected with

**TABLE 1**  
Percentage Growth Inhibition of LNCaP Tumors Treated with  $^{67}\text{Cu}$ -CuSarbisPSMA and  $^{177}\text{Lu}$ -LuPSMA I&T as Compared with Vehicle Control

Group	Growth inhibition (%)	<i>P</i>
$^{67}\text{Cu}$ -CuSarbisPSMA (5 MBq)	58	0.017
$^{177}\text{Lu}$ -LuPSMA I&T (5 MBq)	65	0.007
$^{67}\text{Cu}$ -CuSarbisPSMA (30 MBq)	109	$<0.0001$
$^{177}\text{Lu}$ -LuPSMA I&T (30 MBq)	107	$<0.0001$

Analysis was performed on day 17. *P* values were calculated relative to vehicle control.

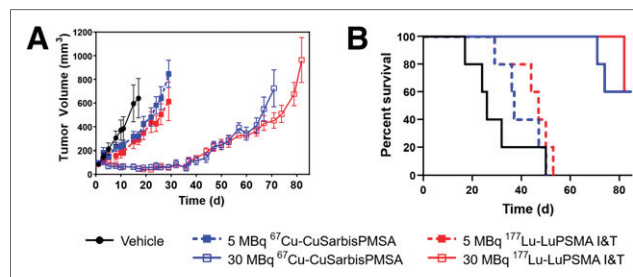


**FIGURE 2.** (A) Inhibition of LNCaP tumor growth after treatment with either  $^{67}\text{Cu}$ -CuSarbisPSMA or  $^{177}\text{Lu}$ -LuPSMA I&T, expressed as mean tumor volume ( $\pm$ SEM) ( $n = 5$ ). (B) Kaplan–Meier curve of percentage survival data; endpoint represents day on which tumor size was at least  $1,200 \text{ mm}^3$  or censoring occurred (day 82).

**TABLE 2**  
Percentage Growth Inhibition of LNCaP Tumors Treated with  $^{67}\text{Cu}$ -CuSarbisPSMA as Compared with Vehicle Control

Group	Growth inhibition (%)	P
7.5 MBq $^{67}\text{Cu}$ -CuSarbisPSMA	100	<0.001
15 MBq $^{67}\text{Cu}$ -CuSarbisPSMA	112	<0.001
30 MBq $^{67}\text{Cu}$ -CuSarbisPSMA	119	<0.001

Analysis was performed on day 13. P values were calculated relative to vehicle control.

$^{67}\text{Cu}$ -CuSarbisPSMA (15 MBq, 0.45  $\mu\text{g}$ , 0.22 nmol) on days 1 and 15 to investigate the potential of fractionated dose protocols. On day 13, tumor growth in each treatment group was suppressed versus the control group (Table 2). All treatments increased survival significantly compared with the vehicle control (7.5 MBq,  $P < 0.001$ ; 15 MBq,  $P < 0.001$ ; 30 MBq,  $P < 0.001$ ). There was a trend for prolonged tumor growth inhibition and survival in the fractionated dose group ( $2 \times 15$  MBq) compared with the single dose (30 MBq), although this was not statistically significant (Fig. 3).

## DISCUSSION

$^{64}\text{Cu}$ -CuSarbisPSMA has excellent uptake in LNCaP tumors in male NSG mice and, importantly, showed excellent retention in the tumor up to 24 h after injection (17), suggesting that the  $^{67}\text{Cu}$  variant may be suited to PSMA-targeted radiotherapy. In this work, we demonstrated that  $^{67}\text{Cu}$ -CuSarbisPSMA and  $^{177}\text{Lu}$ -LuPSMA I&T provide similar tumor inhibition and survival extension at equivalent administered activities. This finding is not surprising, as the energy from the  $\beta^-$  emissions from  $^{67}\text{Cu}$  and  $^{177}\text{Lu}$  are similar. The shorter half-life of  $^{67}\text{Cu}$  than of  $^{177}\text{Lu}$  (61.9 h vs. 6.7 d) means that repeated dosing might be feasible over a shorter time frame, potentially providing better control of rapidly repopulating tumors. Administration of 2 cycles of 15 MBq of activity inhibited tumor growth similarly to a single 30 MBq administration, and although there was a trend for prolonged tumor growth inhibition in the fractionated dose group, the difference was not statistically significant. Further studies could investigate the

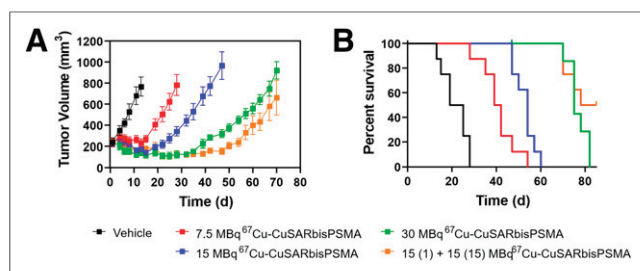


**FIGURE 3.** (A) Antitumor efficacy of  $^{67}\text{Cu}$ -CuSarbisPSMA against LNCaP tumor xenografts, expressed as average tumor size ( $\pm$ SEM) ( $n = 8$ ). (B) Kaplan-Meier curve of percentage survival data; endpoint represents day on which tumor size was at least 1,200  $\text{mm}^3$  or censoring occurred (day 85).

efficacy of administering 4 cycles of 7.5 MBq of activity. The half-life of  $^{67}\text{Cu}$  is similar to that of  $^{90}\text{Y}$  (64.6 h), but with a particulate energy similar to that of  $^{177}\text{Lu}$ . How these physical characteristics might influence therapeutic efficacy in lesions of differing size and biology remains to be determined. Future work will include comparative biodistribution studies quantifying tumor uptake and retention to allow estimates of dose to the tumor and normal tissue.

## CONCLUSION

$^{67}\text{Cu}$ -CuSarbisPSMA is efficacious in the PSMA-expressing LNCaP model of prostate cancer, and further evaluation of the combination of  $^{64}\text{Cu}$ -CuSarbisPSMA and  $^{67}\text{Cu}$ -CuSarbisPSMA as a theranostic approach to prostate cancer is warranted.

## DISCLOSURE

This work was partially funded by Clarity Pharmaceuticals. Paul Donnelly and Carleen Cullinane received funding from the Victorian Cancer Council. Rodney Hicks is a NHMRC Practitioner Fellow (APP1108050). Ellen van Dam and Matthew Harris are employed by Clarity Pharmaceuticals, the licensee of relevant intellectual property. Paul Donnelly and Nicholas Zia are inventors of intellectual property, licensed from the University of Melbourne to Clarity. Paul Donnelly serves on the scientific advisory board of Clarity and has a financial interest. Unrelated to this project, Rodney Hicks has shares in Telix Radiopharmaceuticals, with proceeds donated to his institution. No other potential conflict of interest relevant to this article was reported.

## ACKNOWLEDGMENTS

We thank Dr. Peter Eu for synthesis of  $^{177}\text{Lu}$ -LuPSMA I&T.

## KEY POINTS

**QUESTION:** Is  $^{67}\text{Cu}$ -CuSarbisPSMA therapeutically efficacious?

**PERTINENT FINDINGS:**  $^{67}\text{Cu}$ -CuSarbisPSMA appears as efficacious as an agent already used in clinical practice.

**IMPLICATIONS FOR PATIENT CARE:** Theoretic advantages of the  $^{64}/^{67}\text{Cu}$ -CuSarbisPSMA theranostic pair are the ability to use a chemically identical radiopharmaceutical for treatment selection, dosimetry, and therapy, as well as the shorter half-life of  $^{67}\text{Cu}$  than of  $^{177}\text{Lu}$ , which may allow closer cycles.

## REFERENCES

- Pangalos MN, Neefs J-M, Somers M, et al. Isolation and expression of novel human glutamate carboxypeptidases with N-acetylated  $\alpha$ -linked acidic dipeptidase and dipeptidyl peptidase IV activity. *J Biol Chem.* 1999;274: 8470-8483.
- Afshar-Oromieh A, Babich JW, Kratochwil C, et al. The rise of PSMA ligands for diagnosis and therapy of prostate cancer. *J Nucl Med.* 2016;57(suppl): 79S-89S.
- Kozikowski AP, Nan F, Conti P, et al. Design of remarkably simple, yet potent urea-based inhibitors of glutamate carboxypeptidase II (NAALADase). *J Med Chem.* 2001;44:298-301.
- Hofman MS, Lawrentschuk N, Francis RJ, et al. Prostate-specific membrane antigen PET-CT in patients with high-risk prostate cancer before curative-intent surgery or radiotherapy (proPSMA): a prospective, randomised, multicentre study. *Lancet.* 2020;395:1208-1216.

5. Weineisen M, Schottelius M, Simecek J, et al.  $^{68}\text{Ga}$ - and  $^{177}\text{Lu}$ -Labeled PSMA I&T: optimization of a PSMA-targeted theranostic concept and first proof-of-concept human studies. *J Nucl Med*. 2015;56:1169–1176.
6. Hofman MS, Violet J, Hicks RJ, et al. [ $^{177}\text{Lu}$ ]-PSMA-617 radionuclide treatment in patients with metastatic castration-resistant prostate cancer (LuPSMA trial): a single-centre, single-arm, phase 2 study. *Lancet Oncol*. 2018;19:825–833.
7. Maffey-Steffan J, Scarpa L, Sviridenka A, et al. The  $^{68}\text{Ga}/^{177}\text{Lu}$ -theragnostic concept in PSMA-targeting of metastatic castration-resistant prostate cancer: impact of post-therapeutic whole-body scintigraphy in the follow-up. *Eur J Nucl Med Mol Imaging*. 2020;47:695–712.
8. Hicks RJ. Citius, altius, fortius: an Olympian dream for theranostics. *J Nucl Med*. 2017;58:194–195.
9. Herrmann K, Bluemel C, Weineisen M, et al. Biodistribution and radiation dosimetry for a probe targeting prostate-specific membrane antigen for imaging and therapy. *J Nucl Med*. 2015;56:855–861.
10. Kletting P, Thieme A, Eberhardt N, et al. Modeling and predicting tumor response in radioligand therapy. *J Nucl Med*. 2019;60:65–70.
11. Novak-Hofer I, Schubiger AP. Copper-67 as a therapeutic nuclide for radioimmunotherapy. *Eur J Nucl Med*. 2002;29:821–830.
12. Jackson PA, Beauregard J-M, Hofman MS, Kron T, Hogg A, Hicks RJ. An automated voxelized dosimetry tool for radionuclide therapy based on serial quantitative SPECT/CT imaging. *Med Phys*. 2013;40:112503.
13. DeNardo GL, Kukis DL, Shen S, DeNardo DA, Meares CF, DeNardo SJ.  $^{67}\text{Cu}$ -versus  $^{131}\text{I}$ -labeled Lym-1 antibody: comparative pharmacokinetics and dosimetry in patients with non-Hodgkin's lymphoma. *Clin Cancer Res*. 1999;5:533–541.
14. Cullinane C, Jeffery CM, Roselt PD, et al. Peptide receptor radionuclide therapy with  $^{67}\text{Cu}$ -CuSarTATE is highly efficacious against a somatostatin-positive neuroendocrine tumor model. *J Nucl Med*. 2020;61:1800–1805.
15. Banerjee SR, Pullambhatla M, Foss CA, et al.  $^{64}\text{Cu}$ -labeled inhibitors of prostate-specific membrane antigen for PET imaging of prostate cancer. *J Med Chem*. 2014;57:2657–2669.
16. Hicks RJ, Jackson P, Kong G, et al.  $^{64}\text{Cu}$ -SARTATE PET imaging of patients with neuroendocrine tumors demonstrates high tumor uptake and retention, potentially allowing prospective dosimetry for peptide receptor radionuclide therapy. *J Nucl Med*. 2019;60:777–785.
17. Zia NA, Cullinane C, Van Zuylekom JK, et al. A bivalent inhibitor of prostate specific membrane antigen radiolabeled with copper-64 with high tumor uptake and retention. *Angew Chem Int Ed Engl*. 2019;58:14991–14994.